ELSEVIER

Catalysis Today 56 (2000) 21–34

CATALYSIS TODAY

www.elsevier.com/locate/cattod

Catalytic dehydrogenation of hydrocarbons in palladium composite membrane reactors

P. Quicker [a], V. Höllein [b], R. Dittmeyer [b,*]

[a] *Lehrstuhl für Technische Chemie I, Universität Erlangen-Nürnberg, Egerlandstraße 3, 91058 Erlangen, Germany*
[b] *DECHEMA e.V., Karl-Winnacker-Institut, Theodor-Heuss-Allee 25, 60486 Frankurt am Main, Germany*

Accepted 5 November 1999

Abstract

Different methods for the preparation of hydrogen permselective palladium composite membranes on asymmetric ceramic and porous stainless-steel tubes were tested. Electroless plating, electroplating, chemical and physical vapor deposition, as well as high velocity oxy-fuel spraying were investigated. Electroless plating was confirmed to be a suitable method for coating ceramic supports. Promising methods for the preparation of composite palladium–steel membranes are high velocity oxy-fuel spraying and a combined method of electroplating and electroless plating. Successfully coated membranes were employed for hydrogen separation in lab-scale membrane reactors during the dehydrogenation of ethylbenzene to styrene and propane to propylene. In both cases, the removal of hydrogen significantly increased the olefin yield, as compared to the corresponding conventional packed-bed reactor results. A relative increase of styrene yield above 15% was observed using a palladium–ceramic membrane. The relative increase of propylene yield was close to 18% for the same type of membrane. Employing a stainless steel-based membrane even further increased the yield of propylene. However, in contrast to the virtually defect-free ceramic-based membranes, a certain amount of other components passed the palladium–steel membrane along with hydrogen, amounting to roughly 20% of the total exit gas flow.

Keywords: Membrane reactor; Hydrogen permselective membrane; Composite membrane; Ceramic membrane; Stainless-steel membrane; Dehydrogenation

1. Introduction

The integration of reaction and separation in multifunctional reactor concepts moves more and more to the center of interest of both research institutes and industrial companies. The enormous advantage of such concepts comes — besides of a cost reduction for plant equipment and maintenance and the opportunities of simplified separation and heat management — first of all from the attainment of higher conversion and product yield. This is also the main motivation for applying membrane reactors for hydrocarbon dehydrogenation. Given the removal of hydrogen arising from the dehydrogenation, the reaction can be continued beyond the equilibrium conversion.

However, the use under typically harsh conditions of industrial dehydrogenation processes not only calls for high permeability and high selectivity of the membranes employed, but also for sufficient thermal, mechanical, and chemical stability. Successfully integrating membranes into a reactor design is not a trivial task either. In particular, gastight sealing of ceramic membranes to metallic reactor parts can cause severe difficulties.

* Corresponding author. Fax: +49-9131-857421.
E-mail address: dittmeyer@dechema.de (R. Dittmeyer).

0920-5861/00/$ – see front matter
PII: S0920-5861(99)00259-X

The work so far published in the field of membrane reactors for dehydrogenation of hydrocarbons covers all common reactions and various reactor configurations. Because of the severe demands on the membranes to be employed and the problems raised hereby, experimental investigations carried out under realistic operating conditions are relatively rare. Recent publications deal mainly with modeling and simulation [1] or membrane preparation methods [2–4]. Our work is focused on membrane application for hydrocarbon dehydrogenation, under operating conditions as close to the industrial process as possible. Due to their superior permeance and permselectivity, palladium composite membranes consisting of a thin dense metallic layer on a robust porous support, preferably stainless steel, recommend themselves as most attractive type of membrane for this application. Electroless plating has been described by various authors as a suitable method for coating of thin palladium films on porous ceramic and metal substrates [5,6]. In addition, some work has been reported on other coating techniques as well, e.g. electroplating [7] and chemical vapor deposition [8].

This paper describes preparation and use of palladium composite membranes for two industrially relevant test reactions, i.e. the dehydrogenation of ethylbenzene to styrene and the dehydrogenation of propane to propylene. In the run-up to the membrane reactor tests, extensive kinetic studies were carried out for both reacting systems. A detailed description of the results of the kinetic modeling is beyond the scope of this paper and will be discussed in a separate publication. The kinetic models derived were implemented in a membrane reactor simulation program developed by our group, in order to accompany and facilitate the experimental work [9]. The results of this simulation will also be reported elsewhere [10].

2. Dehydrogenation of hydrocarbons

Heterogeneously catalyzed dehydrogenation reactions are endothermic and equilibrium restricted. In general, the formation of olefins is favored by low pressure (expansion of volume) and high temperature.

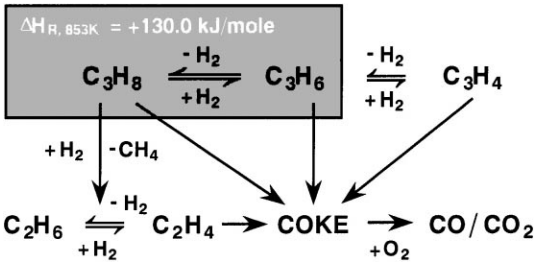

Fig. 1. Simplified reaction scheme for propane dehydrogenation.

2.1. Propane dehydrogenation

During the dehydrogenation of propane to propylene and hydrogen, a series of side reactions take place. The products are shown in Fig. 1. The industrial process is performed in packed bed, moving bed, or fluidized bed reactors at temperatures around 550–650°C and moderate pressure. Frequently, hydrogen is added in quantities of 10–20 mol% in order to delay catalyst deactivation. Common catalysts are Pt–Sn or Cr_2O_3 supported on γ-Al_2O_3 or ZrO_2.

To date membrane reactors for propane dehydrogenation were investigated experimentally only by few authors. Ziaka et al. [11,12] reported the employment of porous alumina membranes with a nominal pore size of 4 nm. The investigations were carried out at ca. 0.2 bar pressure difference between both sides of the membrane, without sweep gas on the permeate side. Using a propane–hydrogen feed (molar ratio 4 : 1), a relative increase of propylene yield of 26% at 90% selectivity to propylene was obtained at 560°C (packed bed: 80%) [11]. Porous membranes were also investigated by Weyten et al. [13]. They could only reach significant improvement of propylene yield at rather low space velocity, i.e. below $0.25\,h^{-1}$ (WHSV). A considerable amount of sweep gas passed the membrane and diluted the reaction mixture (retentate) during the experiments, yet this was not considered responsible for the measured increase in conversion. A patent by Bitter [14] describes the application of porous alumina membranes ($d_{pore} = 10$ nm), e.g. for propane dehydrogenation. It claims improvements of propane conversion from 40.1 to 58.7% (selectivity 90%) at 575°C and a space velocity of $0.5\,h^{-1}$ (WHSV). Collins et al. [15] investigated both porous ceramic membranes ($d_{pore} = 0.5$ nm) and composite

palladium–ceramic membranes. Their experiments were performed at very high space velocity, similar to those in conventional technical reactors. Only with porous membranes an increase of propylene yield was observed. Compared to experiments in a packed-bed reactor the yield was raised from 29.6 to 39.6% with no loss in selectivity but accelerated catalyst deactivation. Under these conditions, the authors found ca. 10 mol% sweep gas in the retentate at the reactor outlet. Employing palladium composite membranes gave a small increase of propylene yield only at low temperature. At temperatures above 560°C propylene yield was even decreased, as compared to experiments in a conventional packed-bed reactor. This was traced back to an instability of the palladium membrane under reaction conditions. Sheintuch and Dessau [16] utilized dense Pd–Ag (76-μm wall thickness) and Pd–Ru tubes (254-μm wall thickness) as membranes for the removal of hydrogen from the dehydrogenation reactor. They reported an enormous improvement of propylene yield. At 550°C, they found a maximum propylene yield of 70%. However, this was achieved at very low space velocity of 0.12 h^{-1} (WHSV).

2.2. Ethylbenzene dehydrogenation

The reaction scheme for ethylbenzene dehydrogenation is shown in Fig. 2. A characteristic feature of this process is the addition of large amounts of steam to the feed. The catalysts used consist first of all of Fe_2O_3 and K_2O. The usual reaction conditions are temperatures in the range of 540–650°C, atmospheric or subatmospheric pressure, a space velocity of 1–2 h^{-1} (WHSV), and a steam-to-oil ratio (s/o) of 0.5–2.0, on a weight basis.

Similar to propane dehydrogenation, the number of publications with experimental matter on the use of membrane reactors for the dehydrogenation of ethylbenzene is rather low. Most of the experimental work carried out deals with porous ceramic membranes. Wu et al. [17] could improve ethylbenzene conversion from 48% (plug flow reactor) to 65% at 640°C by use of ceramic membranes ($d_{pore} = 4$ nm). A slight increase of styrene selectivity was observed. It should be mentioned that these experiments were performed with a feed diluted with nitrogen. Various membrane reactor configurations for porous alumina tubes were investigated by Yang et al. [18]. They reported an absolute increase of styrene yield of 11% at 620°C. Tiscareno-Lechuga and Hill [19] were able to reach the equilibrium conversion of ethylbenzene by employing a porous membrane with a pore size of 5 nm. They had tremendous problems with coking and the low permselectivity of the membrane used. Again, the feed was diluted with nitrogen. A hybrid configuration with a conventional packed-bed reactor followed by a membrane reactor ($d_{pore} = 4$ nm) was investigated by Gallaher et al. [20]. An absolute increase of styrene yield of 7% was achieved. The experiment was performed with a liquid hourly space velocity (LHSV) of 0.4 h^{-1}, a temperature of 575°C and a feed composition $N_2 : H_2O : EB$ of 9 : 9 : 1. Bitter [14] not only proposed the use of porous ceramic membranes for dehydrogenation of propane but also for dehydrogenation of ethylbenzene. At 625°C and 4 bar pressure he reported an improvement of ethylbenzene conversion

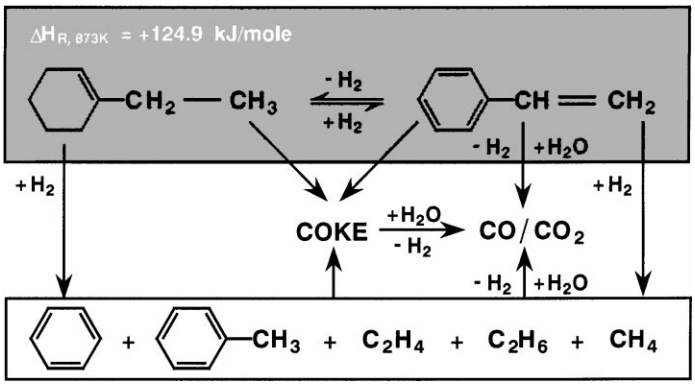

Fig. 2. Simplified reaction scheme for ethylbenzene dehydrogenation.

Table 1
Properties of the membrane supports

	Unit	Sinter metal tubes	Ceramic tubes
Length	(mm)	110	110/150
Outer diameter	(mm)	10	10
Wall thickness	(mm)	2	1.5
Pore size top layer	(μm)	ca. 0.5[a]	0.1[a]
Thickness top layer	(μm)	ca. 100[b]	60[b]
Material		Cr–Ni–Steel	α-Al_2O_3
Manufacturer		Krebsoege GmbH	Inocermic GmbH

[a] Data of manufacturer.
[b] Estimated by SEM-micrographs.

from 50.7 (packed bed) to 65.2% (membrane reactor) at 94% styrene selectivity.

3. Experimental

3.1. Preparation of palladium composite membranes

Asymmetric tubes made of alumina and porous stainless steel, respectively were used as support for the preparation of palladium composite membranes. Both supports consist of a thick macroporous tube and a thin top-layer with small pores on which the palladium was coated. In case of the ceramic tubes the microporous layer is located on the inside, whereas the stainless-steel tubes have it on the outside. The membrane dimensions and other relevant data are summarized in Table 1. SEM-micrographs of both support types are shown in Fig. 3. Electroless plating and chemical vapor deposition (CVD) were employed for the coating of the ceramic supports. The palladium–stainless-steel membranes were prepared by electroless plating, electroplating, physical vapor deposition (PVD), and high velocity oxy-fuel spraying (HVOF).

3.1.1. Electroless plating

The preparation basically was carried according to the method proposed by Collins and Way [2,5]. The support tubes were treated after to the following procedure:

- *Cleaning*: ultrasonic rinsing in ammoniac solution, isopropyl alcohol and deionized water;
- *Surface* sensitizing: immersion in an acidic $SnCl_2/SnCl_4$ bath;

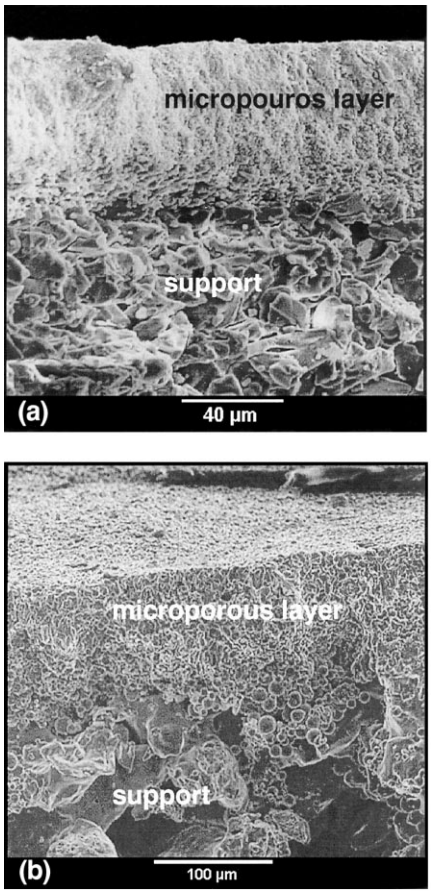

Fig. 3. SEM-micrographs: (a) asymmetric ceramic support; (b) asymmetric porous stainless-steel support.

- *Surface activation*: immersion in an acidic $PdCl_2$ bath;
- *Plating with palladium*: immersion in the electroless-plating bath, with the main components $PdCl_2$ as palladium source and hydrazine (N_2H_5OH) as reducing agent.

The detailed plating instruction can be found in [5]. In the following, the differences between the method of Collins and Way and the plating procedure used in this study are pointed out. In case of the porous stainless-steel tubes, the cleaning sequence was extended by ultrasonic rinsing in acetone to remove adherent contaminants like oil or grease. The carriers were turned upside down after each plating step to avoid the generation of defects at the top end caused by ascending bubbles in the upper part of the tubes.

Drying of the plated membranes at 110°C, at least after every second plating step, proved to be essential for a successful coating, as it greatly improved the adhesive strength of the palladium layer (cf. Chap. 4.1). The ceramic tubes were plated in a length of 150 mm and finally cut to the desired length of 110 mm after preparation. This proved to be advantageous, because the membranes showed defects preferably close to the ends in an area of ca. 10 mm next to the faces. Various attempts to seal the end regions with solder glass, high-temperature cement or similar materials failed. The same holds for sealing of the membrane ends before plating [2], as this prevented a defect-free coating in the transition region between the ceramic tube and the sealing material. Only by cutting off the membrane ends followed by polishing of the faces, a gastight connection of the membrane to the reactor flanges could be established.

3.1.2. Electroplating

The electroplating procedure for the stainless-steel tubes was acquired from a variety of experiments. Above all, the composition of the plating bath, the current density and the plating temperature were investigated. Among others, instructions given by Buxbaum and Hsu [7] for electroplating were picked up. It turned out in the course of the experiments that the best results are obtained by a combination of these plating instructions and the electroless plating procedure described previously. Tube cleaning was carried out analogously to the electroless plating. The same holds for sensitizing and activating of the supports. The actual plating was performed in an acidic palladium chloride solution with ammonia supplemented. Addition of $NaH_2PO_2 \cdot H_2O$, as proposed by Buxbaum and Hsu, was omitted because a better plating control had been achieved without. The constituents of the electroplating bath are listed in Table 2. The plating was carried out at temperatures of 50–60°C with 0.1–0.5 mA cm^{-2} current density. Higher current densities and temperatures reduced the adhesive strength and the durability of the palladium layer. After plating, the membranes were rinsed in deionized water and dried at 110°C for several hours.

Table 2
Electroplating bath composition

Substance	Formula	Concentration
Palladium(II)-chloride	$PdCl_2$	2 g l^{-1}
Hydrochloric acid	HCl (38%)	4 ml l^{-1}
Ammonium hydroxide	NH_4OH	160 ml l^{-1}

Table 3
Operating conditions chemical vapor deposition

Parameter	Unit	Value
Vaporizer temperature	(°C)	60
Reactor temperature	(°C)	210
Reactor pressure	(Pa)	50000
Feed mass flow	(mg min^{-1})	0.4
Gas flow N_2	(N ml min^{-1})	111
Residence time	(s)	9.5
Deposition time	(h)	9–11

3.1.3. Chemical vapor deposition (CVD)

CVD was studied as another potential method to coat the ceramic tubes. Membrane cleaning was again performed corresponding to the electroless-plating procedure. Palladium hexafluoroactylacetonate $Pd(C_5HF_6O_2)_2$ was used as palladium precursor. The precursor was vaporized at 60°C and fed to the CVD-reactor using nitrogen as carrier gas. There it was decomposed at 210°C and palladium was deposited on the ceramic tubes fixed inside the reactor. The shell side and the faces of the tubes were sealed so that they could not get in touch with palladium. Similar to the electroless plating, the tubes were turned upside down after half of the deposition time to ensure a uniform coating. The CVD deposition parameters are summarized in Table 3.

3.1.4. Physical vapor deposition (PVD)

PVD was used to coat porous stainless-steel tubes only. In this technique, Pd is evaporated in a vacuum chamber and subsequently deposited by condensation on the surface of the support placed inside the vacuum chamber. Several PVD-versions are commonly used. The experiments reported here have been carried out using an electron beam evaporation instrument at the Institute for Solid State and Materials Research Dresden (Germany), which was operated below 1×10^{-5} mbar pressure. Pd was charged in a crucible inside the vacuum chamber. The stainless-steel tube rotated roughly 7 cm above the

crucible inside the vacuum chamber. The temperature of the support was controlled. Coating experiments were carried out at support temperatures around 250°C and deposition rates in the range of 1–3 nm s^{-1}.

3.1.5. High velocity oxy-fuel spraying (HVOF)

The coating by high velocity oxy-fuel spraying was carried out in cooperation with ATZ EVUS, Vilseck (Germany). HVOF is a thermal spraying technique for coating of supports based on powder-type spraying materials. The Pd powder is partly molten in an oxygen-fuel flame at temperatures of 2600–2900°C and sprayed on the support using high spraying velocities in the range of 500–600 m s^{-1}. At the surface, the impinging particles are deformed due to their high thermal and kinetic energy. Repeated coating finally leads to a continuous Pd layer.

The palladium powder used was provided by Degussa AG in a grain size below 45 μm. A propane/air mixture served as a fuel for the spray gun. After cleaning with ethanol, the tube was clamped horizontally and set into rotation around its longitudinal axis. During the coating, the spray gun was moved computer-controlled along the rotating tube at linear velocities of 25 and 37 mm s^{-1}, respectively. This procedure was repeated several times until the desired thickness of the palladium layer was reached.

3.2. Dehydrogenation experiments

Identical membrane reactors were used for both test reactions. The construction details of the reactor are shown in Fig. 4. Essentially, the reactor consists of two concentric tubes with a length of 110 mm which are clamped between two metal flanges and sealed by graphite seals. The inner tube is the composite membrane, the outer one is a dense tube of the same material as the membrane support. The catalyst is filled into the annular space between the membrane and the dense tube. Commercial catalysts were employed for both reactions.

Two separate test rigs were set up for propane and ethylbenzene dehydrogenation, respectively. The one used for propane dehydrogenation besides the reactor includes thermal mass flow controllers as gas feeding devices for propane, hydrogen, nitrogen, and synthetic air. Alternatively the feed (C_3H_8, H_2, N_2) or

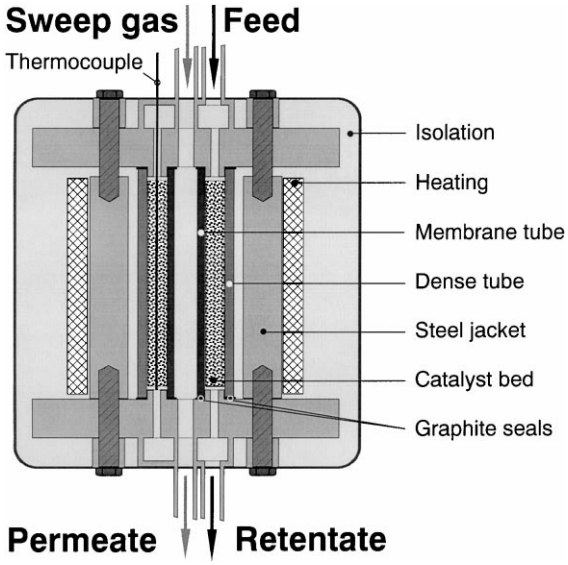

Fig. 4. Construction principle of the laboratory membrane reactor.

a regeneration gas (N_2, synth. air) can be supplied. Hydrogen removal at the permeate side of the reactor can be realized by nitrogen sweep gas or by using a vacuum pump (Vacuubrand, MD 4C). Pressure controllers for shell and tube side are installed. A gas chromatograph (Dani, 86.10) equipped with flame ionization (FID) and thermal conductivity (TCD) detectors serves for product analysis. The apparatus for dehydrogenation of ethylbenzene is equipped with liquid pumps for dosage of ethylbenzene and water, a vaporizer and two condensers for the exit gas streams (retentate and permeate side). Condensable hydrocarbons are analyzed by a FID (Siemens RGC 202), the gaseous components are determined by a TCD and, after methanization, additionally by a FID. Thermal mass flow controllers for dosage of sweep gas and a pump (Vacuubrand, cvc 2000) for evacuating the permeate side complete the experimental setup.

4. Results and discussion

4.1. Results of membrane preparation

4.1.1. Composite palladium–ceramic membranes

By electroless-plating porous ceramic tubes were coated with defect-free palladium layers in

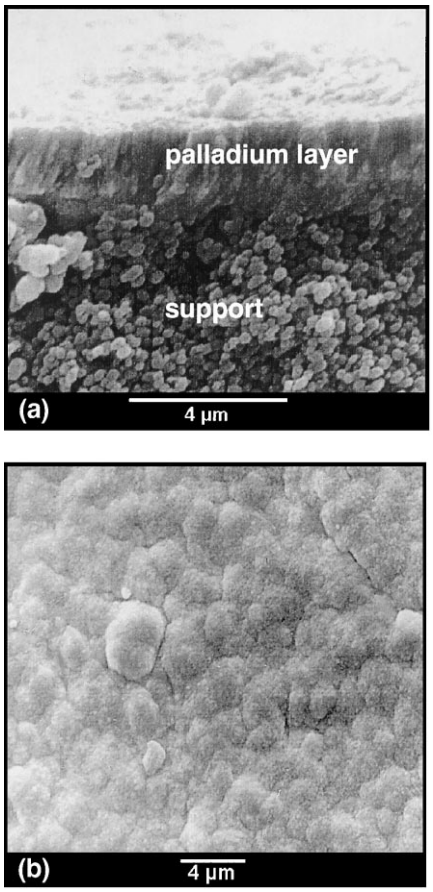

Fig. 5. SEM-micrographs of a composite palladium–ceramic membrane prepared by electroless plating: (a) cross section; (b) palladium surface.

reproducible manner. Layers with a thickness of 0.3–0.4 μm could be deposited in one plating step. The palladium layers have a very good adherence on the support. Fig. 5 shows the cross section and the surface of a membrane after six plating steps. It is clearly visible that the palladium is firmly connected to the ceramic support. The palladium layer is ca. 2–3 μm thick. The membrane surface shows the typical palladium clusters which are perfectly grown together in this case; defects are absent. Membranes prepared according to this procedure have a hydrogen permeance of ca. 4×10^{-7} mol m^{-2} s^{-1} Pa^{-1} at temperatures representative for dehydrogenation reactions (400–600°C). In this temperature range, no significant dependence of the permeance on temperature was observed as shown in Fig. 6. In contrast,

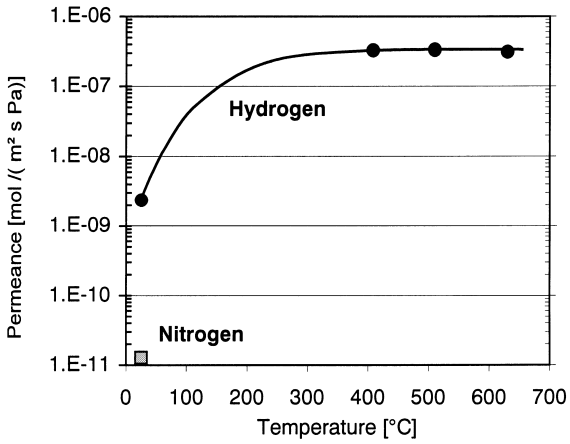

Fig. 6. Hydrogen and nitrogen permeance of electroless plated composite palladium–ceramic membranes.

the value of 2.5×10^{-9} mol m^{-2} s^{-1} Pa^{-1} determined at room temperature is much lower. The permeance of nitrogen at room temperature was found to be 10^{-11} mol m^{-2} s^{-1} Pa^{-1}, resulting in an ideal separation factor for H_2/N_2 of 250. Measurements of nitrogen permeance at elevated temperature were not performed yet. However, higher separation factors are expected due to the increase of hydrogen permeance with temperature.

Table 4 shows a comparison of the hydrogen permeance and permeability of the prepared membranes with selected data from literature. Despite the lower thickness of the palladium layer the composite membranes prepared in this study exhibit a lower hydrogen permeance. The difference in hydrogen permeability based on the thickness of the Pd layer as derived from SEM-micrographs is therefore even more striking. So far no detailed explanation can be given for these findings. It is assumed that Pd is also deposited beyond the surface, i.e. inside the pores of the ceramic top-layer, consequently pretending a lower thickness.

In the run-up to the dehydrogenation experiments the thermal stability of the membranes was tested. Fig. 7a shows a membrane prepared by electroless plating after heating to 620°C for more than 70 h in presence of air. No defects are visible. Measurements of nitrogen permeability before and after the temperature treatment gave identical results. Fig. 7b shows a view on the surface of a membrane after heating to 850°C for a duration of 2 h. In this case, holes in the palladium

Table 4
Comparison of the permeation results of the palladium–ceramic membranes prepared by electroless plating with selected literature data

Temperature (°C)	Thickness of the Pd film (μm)	H_2 permeance ($mol\,m^{-2}\,s^{-1}\,Pa^{-1}$)	H_2 permeability ($mol\,m^{-1}\,s^{-1}\,Pa^{-1}$)	Separation factor (H_2/N_2)	Coating method	Reference
25	3	3×10^{-9}	9×10^{-15}	>300	Electroless plating	This work
400–600	3	4×10^{-7}	1.2×10^{-12}	>300	Electroless plating	This work
500	8	5×10^{-6}	4.0×10^{-11}	>1000	CVD	Yan et al. [21]
500	12	8×10^{-7}	9.6×10^{-12}	770	Electroless plating	Collins et al. [15]

layer are clearly visible. Moreover, the structure of the layer has been changed to more or less isolated palladium clusters. Normally, individual palladium clusters are hardly visible. Testing of this membrane against nitrogen overpressure showed remarkable leakage.

During the electroless-plating experiments it was found that drying of the membranes, at least after every second plating step, is essential for the formation of defect-free layers. Initial drying of the membranes yet after the whole plating procedure led in most cases to the formation of cracks in the palladium layer. It is assumed that during the plating some water is trapped inside the palladium layer. When this water is evaporated during the final heating it may generate cracks. Intermediate drying at 110°C reduces the risk of crack formation since the amount of trapped water should be reduced.

The preparation of compact palladium films by CVD did not have the expected success yet. It was noticed that palladium was deposited preferably in the pores of the ceramic support. Although the presence of palladium was reaffirmed by weight increase and EDX analysis, SEM-micrographs of the membrane surface hardly showed a difference compared with the bare support. Obviously the pore size of the ceramic supports employed has been too large, so that the precursor could deeply penetrate into the bulk structure of the support before the deposition occurred. Ongoing experiments carried out with ceramic tubes with reduced pore diameter of 4 nm showed already improved results.

4.1.2. Composite palladium–stainless-steel membranes

Porous stainless-steel membranes were coated by palladium using a combination of electroless and electroplating, HVOF, and PVD.

It was found that electroless plating of Pd on porous stainless-steel tubes, when compared to the use of ceramic tubes, leads to similar deposition rates. However, many defects in the palladium layer remained even after numerous plating steps. Dense palladium films could neither be established by electroplating alone, because of too low plating rates (roughly 0.1–0.2 $\mu m\,h^{-1}$). Electroless plating followed by

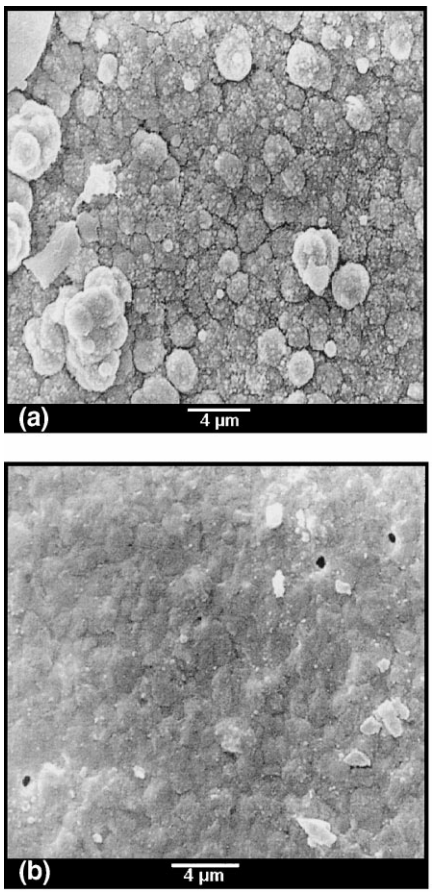

Fig. 7. SEM-micrographs; effect of temperature treatment on electroless plated composite palladium–ceramic membranes: (a) 620°C, 70 h; (b) 850°C, 2 h.

electroplating was the only method producing plane and coherent palladium layers, although the success of this method turned out to be dependent on the structure of the support. Only stainless-steel tubes sintered at relatively high temperature proved to be suitable. High sintering temperatures guarantee a plane and nearly smooth surface. But even through the use of this type of supports and the combination of electroless and electroplating techniques the quality of the ceramic-based composite membranes could not yet be reached. In Fig. 8, the nitrogen permeance of various palladium–stainless-steel membranes is compared with that of a palladium–ceramic membrane. The stainless-steel membrane coated by combined plating shows a nitrogen permeance about two orders of magnitude higher than the ceramic-based membranes. The palladium surface is shown in Fig. 9. The palladium clusters are well grown together, no defects are visible. Obviously, the measured larger nitrogen permeance must be due to single defects of the stainless-steel support which cannot be covered by this coating method. Fig. 10 shows an example of such a defect found in the top layer of a porous stainless-steel tube. It is clear that a coating of defects of nearly 50 μm size is hardly possible.

The surface of a PVD-coated stainless-steel tube is shown in Fig. 11. The palladium clusters do not yet form a coherent layer, there is still some space left between. This is confirmed by the nitrogen permeance (cf. Fig. 8). Values of about $1.5 \times 10^{-8}\,\mathrm{mol\,m^{-2}\,s^{-1}\,Pa^{-1}}$ were measured.

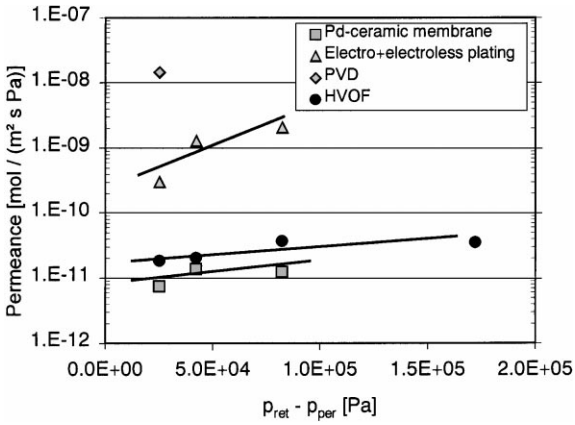

Fig. 8. Nitrogen permeance of various coated palladium composite membranes.

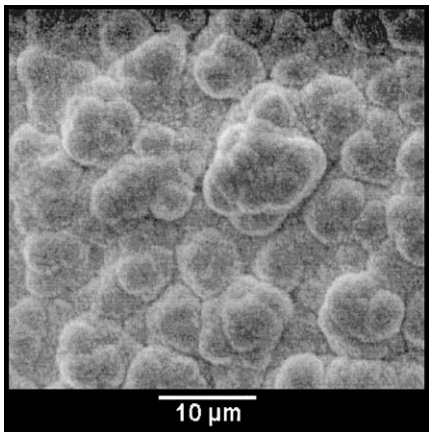

Fig. 9. SEM-micrograph of a composite palladium–stainless-steel membrane prepared by a combination of electroplating and electroless plating.

Compared to the palladium–ceramic membranes this is more than three orders of magnitude higher.

The best preparation results for the stainless-steel-based membranes were obtained by HVOF. As can be seen in Fig. 8, the nitrogen permeance almost reaches the low level of the palladium–ceramic membranes. However, the layers coated by HVOF are considerably thicker, e.g. the palladium layer shown in Fig. 12a has a thickness of roughly 70 μm. As demonstrated clearly by the transparent cut shown in Fig. 12b, the layer is coherent and no open pores exist. For the preparation by HVOF symmetric porous stainless-steel tubes were used. These supports have a pore diameter consider-

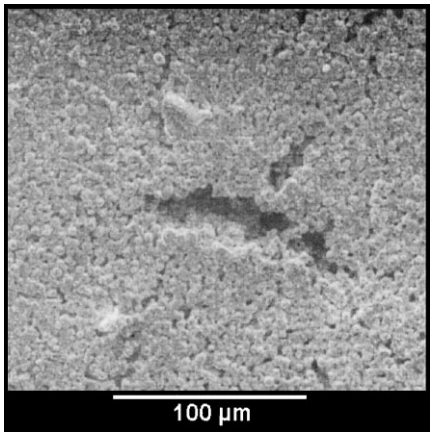

Fig. 10. SEM-micrograph of a defect in the top layer of an asymmetric porous stainless-steel support.

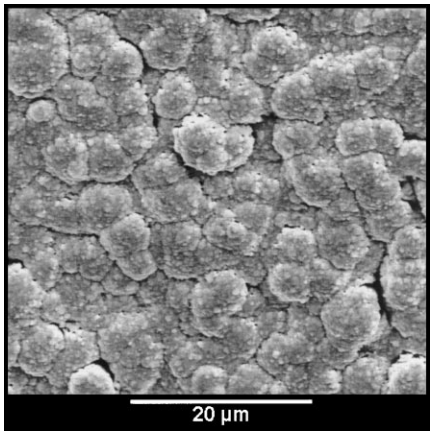

Fig. 11. SEM-micrograph of a composite palladium–stainless-steel membrane prepared by physical vapor deposition.

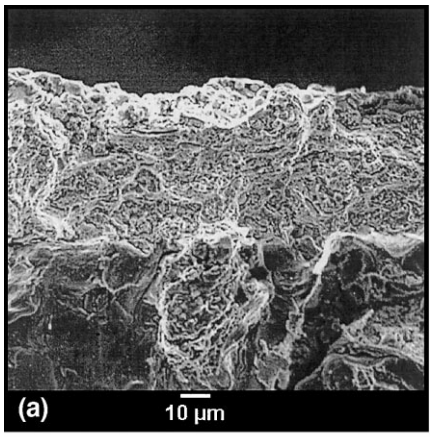

Fig. 12. Composite palladium–stainless-steel membrane prepared by high velocity oxy-fuel spraying: (a) SEM-micrograph; (b) transparent cut.

Table 5
Operating conditions of propane dehydrogenation

Parameter	Unit	Value
Reactor temperature	(°C)	560
Retentate pressure	(Pa)	130 000
Permeate pressure	(Pa)	110 000
GHSV	($Nl\,l^{-1}\,h^{-1}$)	200
Normalized sweep gas flow	(–)	17
Catalyst weight	(g)	7.0
Catalyst grain size	(mm)	0.8–1.0

ably larger and less uniform than the top-layer of the asymmetric supports. It is therefore expected that the use of asymmetric tubes together with fine Pd spraying powders will allow to prepare palladium layers of reduced thickness with the same quality. This is desirable with regard to an increased hydrogen flux.

4.2. Results of the dehydrogenation experiments

4.2.1. Dehydrogenation of propane

For membrane reactor experiments on the dehydrogenation of propane composite palladium–ceramic and composite palladium–stainless-steel membranes were used. The ceramic membrane was prepared by six steps of electroless plating. The resulting palladium film had a mean thickness of 2.3 µm. The stainless-steel membrane was coated by combined electroless plating and electroplating, resulting in 8 µm thickness of the palladium layer. The conditions and parameters for the experiments are summarized in Table 5. The normalized sweep gas flow φ was calculated as follows:

$$\varphi = \frac{\dot{n}_{N_2}/A_{perm}}{\dot{n}_{C_3H_8}/(A_{ret}\varepsilon_b)} \quad (1)$$

Propane conversion (X) and product yields (Y_i) were calculated by the use of the following equations:

$$X_{C_3H_8} = \frac{\dot{n}^{in}_{C_3H_8} - (\dot{n}^{out,ret}_{C_3H_8} + \dot{n}^{out,perm}_{C_3H_8})}{\dot{n}^{in}_{C_3H_8}} \times 100\,(\%) \quad (2)$$

$$Y_i = \frac{\dot{n}_i^{out,ret} + \dot{n}_i^{out,perm}}{\dot{n}^{in}_{C_3H_8}} \times 100\ (\%) \quad (3)$$

The results discussed in this paper refer to the activity of the fresh catalyst. According to the experience from

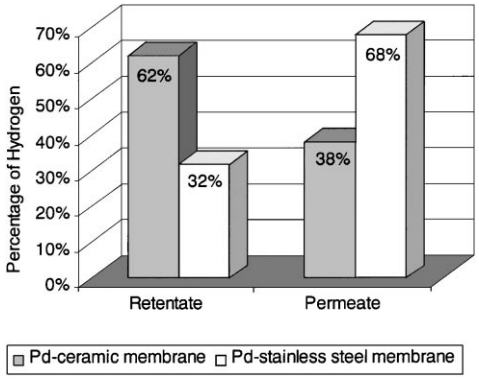

Fig. 13. Proportion of hydrogen measured in retentate and permeate during the propane dehydrogenation experiments.

the kinetic investigations, the activity of the catalyst is virtually constant only for the first 1–2 h. Then, it decreases because of catalyst deactivation due to coking.

Decisive for the increase of propane conversion and propylene yield in the membrane reactor is the rate of hydrogen transport through the membrane. Fig. 13 shows the percentage share of hydrogen determined in the permeate and retentate streams for both types of membranes investigated. Despite the larger palladium layer thickness of the stainless-steel-based membrane, a higher hydrogen permeance of 3.8×10^{-7} mol m^{-2} s^{-1} Pa^{-1} was observed, as compared to the value measured for the ceramic-based membrane of 1.5×10^{-7} mol m^{-2} s^{-1} Pa^{-1}. The obvious reason for this are defects of the palladium layer of the stainless-steel-based membrane. This was confirmed by the observation of product gases other than hydrogen in the sweep gas, amounting to roughly 15–25% of the total product gas. Within measurement accuracy, no product gases were detected in the sweep gas during the experiments with the palladium–ceramic membranes. However, the hydrogen permeability of the palladium–ceramic membrane calculated from the results of the dehydrogenation experiments was about three times lower than the value obtained from the separate permeation experiments. In Fig. 14, the conversion of propane and the product yields determined from the membrane reactor tests are compared to the corresponding values of a conventional packed-bed reactor experiment. The yields of propylene, ethylene and ethane for the experiment with the palladium–stainless-steel membrane are not given, because they could not be quantified accurately due to the high dilution in the sweep gas. The figure also shows the conversion

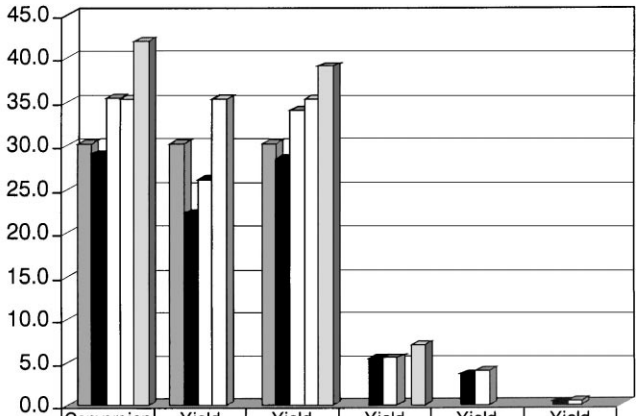

	Conversion Propane	Yield Propylene	Yield Hydrogen	Yield Methane	Yield Ethane	Yield Ethylene
Equilibrium (calc.)	30.2	30.2	30.2	-	-	-
Packed Bed	29.0	22.2	28.5	5.4	3.6	0.4
Pd-ceramic membrane	35.4	26.1	34.0	5.5	4.0	0.5
Pd-ceramic membrane (sim.)	35.3	35.3	35.3	not incl.	not incl.	not incl.
Pd-stainless steel membrane	42.0	not det.	39.0	7.0	not det.	not det.

Fig. 14. Conversion and product yields of the propane dehydrogenation experiments.

Table 6
Operating conditions of ethylbenzene dehydrogenation

Parameter	Unit	Value
Reactor temperature	(°C)	580
Retentate pressure	(Pa)	110 000
Permeate pressure	(Pa)	100 000
WHSV	($kg\,kg^{-1}\,h^{-1}$)	1
S/O	($kg_{H_2O}\ kg_{EB}^{-1}$)	2
Normalized sweep gas flow	(–)	0–105
Catalyst weight	(g)	20.0
Catalyst grain size	(mm)	0.8–1.0

of propane which was calculated by the simulation program for the conditions of the experiment with the palladium–ceramic membrane [9]. Furthermore, the calculated equilibrium conversion is given (Aspen Plus). In the simulation and for the equilibrium calculation only the main reaction was considered.

As expected, both propane conversion and propylene yield obtained in the experiment with the palladium–ceramic membrane are higher than the values determined in the conventional packed-bed reactor. The yield of propylene increased from 22.2 (packed-bed reactor) to 26.1% (Pd–ceramic membrane reactor). Due to the larger amount of hydrogen removed through the palladium–stainless-steel membrane (cf. Fig. 13), the conversion obtained in this test was even higher. The hydrogen yield increased from 34.0 (Pd–ceramic membrane) to 39.0% (Pd–stainless-steel membrane), the conversion from 35.4 to 42%. Compared to the palladium–ceramic membrane this represents a relative increase of propane conversion of 37.5%, compared with the packed-bed reactor even 44.8 %. Due to an increased formation of byproducts the propylene selectivity is slightly reduced.

It should also be mentioned that the conversion calculated from the membrane reactor model fits well to the experimental value.

4.2.2. Dehydrogenation of ethylbenzene

The dehydrogenation of ethylbenzene to styrene was investigated in the laboratory membrane reactor using a palladium–ceramic membrane prepared by electroless plating, having a palladium layer thickness of 2.4 μm. The operating conditions for the experiment are listed in Table 6. The normalized sweep gas flow, the conversion of ethylbenzene, and the product yields were calculated according to Eqs. (1)–(3). The dehydrogenation experiment was started in conventional packed-bed mode, i.e. the permeate side was shut off before and behind the reactor by valves. After the initial forming phase of the catalyst and reaching of a steady state, the permeate side was opened and sweep gas (nitrogen) was supplied. Fig. 15 shows the hydrogen flow measured at the outlet of shell and tube side of the reactor as a function of the normalized sweep gas flow. The hydrogen values for sweep gas flows of 83.6 and 104.5 are not included because as a matter of the high dilution the concentration of hydrogen dropped to very small values which could not be quantified with reasonable accuracy. The amount of hydrogen on the permeate side increased with increasing sweep gas flow. This is an obvious effect of

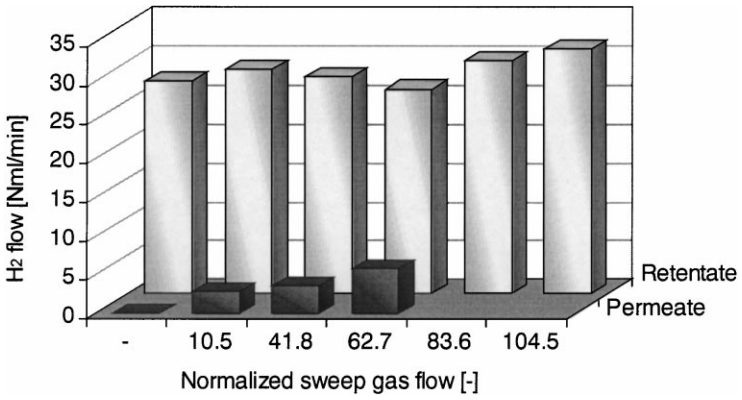

Fig. 15. Hydrogen flow in retentate and permeate during the ethylbenzene dehydrogenation experiments.

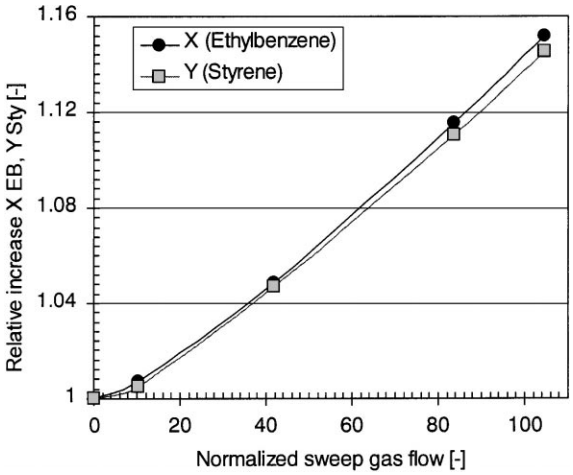

Fig. 16. Relative increase of ethylbenzene conversion and styrene yield as a function of the normalized sweep gas flow.

the reduced partial pressure of hydrogen at the sweep gas side. Note that the percentage of removed hydrogen in this experiment was much lower than during the propane dehydrogenation experiment (Fig. 13). This can be traced back to the lower hydrogen partial pressure during the ethylbenzene dehydrogenation experiment, caused by the large amount of steam present in the feed. The amount of hydrogen in the retentate appears to be hardly affected by the sweep gas flow. At high sweep gas flow even a slight increase of the hydrogen flow was determined. Obviously, the reaction is able to supply enough hydrogen to keep the hydrogen level constant or even increase it slightly. This was confirmed by the measured conversion of ethylbenzene and the yield of styrene. The relative increase of both values, as a function of the normalized sweep gas flow, is shown in Fig. 16. The maximum increase, obtained at the highest sweep gas flow, reached ca. 15%. The course of the curves even points to a further increase when applying even higher sweep gas flows. Due to limitations of the apparatus this could not be shown so far. A minimal loss of styrene selectivity (93.5–93%) was caused by a slight increase of the byproducts toluene and methane.

5. Conclusion

Composite palladium–ceramic membranes with good hydrogen permeability and permselectivity were prepared by electroless plating. The membranes were stable at least for roughly 100 h at temperatures up to 620°C. For coating of porous stainless-steel supports various methods were tested. HVOF and a combination of electroless and electroplating were identified as the most promising methods so far. Both preparation methods have still to be improved and optimized. In the case of HVOF a thickness reduction of the palladium layer by a factor of 2–4 appears to be possible when using fine spraying powders and improved supports. For the combined method of electroplating and electroless plating above all the quality of the porous sinter metal supports has to be improved. The test of the composite membranes in dehydrogenation experiments as well as in permeance measurements gave encouraging results which are qualitatively in agreement with literature.

6. Symbols

A	flow area (retentate or permeate side) (m^2)
ε_b	packed-bed voidage (–)
φ	normalized sweep gas flow (–)
$\dot{n}_i$	mole flow of species i (kmol h^{-1})
s/o	steam-to-oil ratio (weight basis) (–)
WHSV	weight hourly space velocity (h^{-1})
X	conversion (%)
Y_i	yield of product i(%)

Indices

in	feed
out	product
perm	permeate
ret	retentate

Acknowledgements

The authors thank the Bavarian Catalysis Research Network FORKAT for financial support, Linde AG and Süd-Chemie AG for excellent cooperation, GKN Sinter Metals Filters GmbH and Inocermic GmbH for the supply with membrane supports and the Institute for Solid State and Materials Research Dresden and ATZ EVUS Vilseck for their preparation work.

References

[1] Y.L. Becker, A.G. Dixon, W.R. Moser, Y.H. Ma, J. Membr. Sci. 77 (1993) 233.
[2] J.P. Collins, J.D. Way, Ind. Eng. Chem. Res. 32 (1993) 3006.
[3] K.L. Yeung, A. Varma, AIChE J. 41 (1995) 2131.
[4] S. Uemiya, M. Kajiwara, T. Kojima, AIChE J. 43 (1997) 2715.
[5] J.P. Collins, J.D. Way, US Patent Application, 5,451,386 (1995).
[6] P.P. Mardilovich, Y. She, Y.H. Ma, M.H. Rei, AIChE J. 44 (1998) 310.
[7] R.E. Buxbaum, P.C. Hsu, US Patent Application, 5,149,420 (1992).
[8] G. Xomeritakis, Y.S. Lin, AIChE J. 44 (1998) 174.
[9] Ch. Hermann, P. Quicker, R. Dittmeyer, J. Membr. Sci. 136 (1997) 161.
[10] R. Dittmeyer, V. Höllein, P. Quicker, 1st International Symposium on Multifunctional Reactors, Amsterdam, 25–28 April 1999.
[11] Z.D. Ziaka, R.G. Minet, T.T. Tsotsis, AIChE J. 39 (1993) 526.
[12] Z.D. Ziaka, R.G. Minet, T.T. Tsotsis, J. Membr. Sci 77 (1993) 221.
[13] H.D. Weyten, K. Keizer, J. Luyten, R. Leysen, Proc. 4th Workshop Optimisation of Catalytic Membrane Reactor Systems, Oslo, 30–31 May 1997.
[14] J.G.A. Bitter, UK Patent Application, 2,201,159 A (1986).
[15] J.P. Collins, R.W. Schwartz, R. Sehgal, T.L. Ward, C.J. Brinker, G.P. Hagen, C.A. Udovich, Ind. Eng. Chem. Res. 35 (1996) 4398.
[16] M. Sheintuch, R.M. Dessau, Chem. Eng. Sci. 51 (1996) 535.
[17] J.C.S. Wu, T.E. Gerdes, J.L. Pszczolkowski, R.R. Bhave, P.K.T. Liu, Sep. Sci. Tech. 25 (1990) 1489.
[18] W.-S. Yang, J.-C. Wu, L.-W. Lin, Catal. Today 25 (1995) 315.
[19] F. Tiscareno-Lechuga, C.G. Hill Jr., Appl. Catal. A. 96 (1993) 33.
[20] G.R. Gallaher Jr., G.R.T.E. Gerdes, P.K.T. Liu, Sep. Sci. Tech. 28 (1993) 309.
[21] S. Yan, H. Maeda, K. Kusakabe, S. Morooka, Ind. Eng. Chem. Res. 33 (1994) 616.